

Effects of Renal Denervation on Gap Junction in High-Pacing-Induced Heart Failure Dogs

ABSTRACT

Background: Gap junction remodeling is an important cause of ventricular arrhythmia in heart failure. However, it remains unclear whether renal denervation (RDN) regulates gap junction remodeling in heart failure. To explore the effect of RDN on gap junction remodeling in dogs with high-pacing-induced heart failure.

Methods: Fifteen dogs were randomly divided into control (n = 5), heart failure (HF) (n = 5), and RDN+HF (n = 5) group. A high-pacing-induced-heart failure model was established using rapid right ventricular pacing for 4 weeks. The RDN+HF group underwent surgical and chemical ablation of both renal arteries before 4 weeks rapid right ventricular pacing. After 4 weeks, echocardiography, High-Performance Liquid Chromatography-Mass Spectrometry test for norepinephrine and epinephrine, and pathological analysis were performed in the above 3 groups. Further, immunohistochemical staining was used to detect tyrosine hydroxylase, ChAT, connexin 43 (Cx43), and connexin 40 (Cx40). Connexin 43 and Cx40 expression was detected by western blotting. Transmission electron microscopy was used to observe the gap junction.

Results: Compared to the control group, myocardial fibrosis and sympathetic hyperactivity were observed in the HF group. Immunohistochemical staining and western blotting showed that Cx40 expression and Cx43 expression was significantly reduced in the HF group. Compared with the HF group, the RDN+HF group showed reduced sympathetic hyperactivity, Cx40 expression, Cx40/Cx43 ratio, and increased Cx43 expression.

Conclusion: Renal denervation alleviates gap junction remodeling in high-pacing-induced heart failure dogs.

Keywords: Heart failure, renal denervation, sympathetic activity, gap junction, connexin 43

INTRODUCTION

Heart failure (HF) is the leading cause of cardiovascular disorders.¹ Over half of individuals with HF ultimately succumb to ventricular arrhythmia.² Nevertheless, there remains a dearth of efficacious medications for managing ventricular arrhythmia in HF.³ Renal denervation (RDN) has emerged as a prospective approach in addressing arrhythmia in HF. Furthermore, the mechanisms underlying the potential antiarrhythmic properties of RDN are yet to be elucidated.

Remodeling of gap junctions has been identified as a key factor in the development of ventricular arrhythmias during HF.^{3,4} Prior research has demonstrated that there is ongoing restructuring of the gap junctions with cardiomyocytes in HF.^{3,4} These alterations result in an increased vulnerability to ventricular arrhythmias.^{5,6} Several investigations have proposed a significant association between the activation of the renin–angiotensin–aldosterone (RASS) system and the remodeling of the gap junctions.⁷ Thus, the primary objective of this study was to investigate the impact of RDN on gap junction remodeling in HF induced by high pacing.

Heart failure is the most predominant cause of cardiovascular conditions. Over half of individuals with HF ultimately succumb to ventricular arrhythmia. Nonetheless, there remains a shortage of effective medications for managing ventricular arrhythmia in HF. Recently, research into RDN has emerged as a promising

ORIGINAL INVESTIGATION

Xiaoyan Liang^{1,2} 

Shuai Shang^{1,2} 


Zechen Bai³ 

Qing Wang^{1,2} 

Yongqiang Fan⁴ 

Jiasuoer Xiaokereti^{1,2} 

Huasheng Lv^{1,2} 

Xianhui Zhou^{1,2} 

Yanmei Lu^{1,2} 

Baopeng Tang^{1,2} 

¹Department of Pacing and Electrophysiology, The First Affiliated Hospital of Xinjiang Medical University, Xinjiang, China

²Xinjiang Key Laboratory of Cardiac Electrophysiology and Cardiac Remodeling, The First Affiliated Hospital of Xinjiang Medical University, Xinjiang, China

³Department of Medical Engineering and Technology, Xinjiang Medical University, Xinjiang, China

⁴The Fifth Affiliated Hospital of Jinan University (Heyuan Shenhe People's Hospital), Guangdong, China

Corresponding author:

Baopeng Tang
✉ tangbaopeng1111@163.com

Received: October 10, 2023

Accepted: May 6, 2024

Available Online Date: July 12, 2024

Cite this article as: Liang X, Shang S, Bai Z, et al. Effects of renal denervation on gap junction in high-pacing-induced heart failure dogs. *Anatol J Cardiol*. 2024;28(9): 429–436.



Copyright©Author(s) - Available online at anatoljcardiol.com.
Content of this journal is licensed under a Creative Commons Attribution-NonCommercial 4.0 International License.

DOI:10.14744/AnatolJCardiol.2024.3871

approach for addressing arrhythmia in HF. Yet the mechanisms underlying the potential antiarrhythmic impacts of RDN are yet unknown. Gap junction rearrangement has been identified as a key factor in ventricular arrhythmia accompanying HF.⁸ Studies have noted ongoing rearrangements in cardiomyocyte gap junctions in HF,^{3,4} which heighten susceptibility to ventricular arrhythmia.^{5,6} Some investigations have proposed a notable association between the activation of the renin–angiotensin–aldosterone system (RAAS) and gap junction remodeling.^{5,7} Hence, the objective of this study was to investigate the impact of RDN on gap junction remodeling in high-pacing-induced HF.

METHODS

Animals and Welfare

All dogs (weight 12–15 kg, male or female, age 1–2 years old) were raised in an SPF laboratory (temperature, 22–26°C; humidity, 50–70%, light–darkness cycle, 12 hours light, 12 hours darkness; unlimited food and water) and were randomly divided into 3 groups, including the control (n=5), HF (n=5), and RDN+HF (n=5) group. There was no pacemaker implantation and RDN in the control group. The HF group received 4 weeks of rapid right ventricular pacing (RVP). The RDN+HF group underwent RDN before RVP. The study was approved (IACUC-201902-K03) and was carried out strictly in accordance with the Declaration of Helsinki. At the end of the study, the dogs were euthanized by an anesthetic overdose. Blood, renal, and heart tissues were harvested for further analysis (Figure 1).

Construction of High-Pacing-Induced Heart Failure Model

The construction of a high-pacing-induced HF dog model was described in our previous study.⁸ In brief, the cork-screw electrode was inserted under ultrasound guidance, implanted in the apex of the right ventricle, and connected to a cardiac pacemaker. After 2 weeks of recovery, pacemaker frequency was adjusted to RVP (180 bpm for 3 days, 220 bpm for 3 days, and 250 bpm for 3 weeks). Heart failure was defined as left ventricular ejection fraction (EF) less than 45%. Serum B-type natriuretic peptide (BNP) was determined using a BNP ELISA kit (Jianglai, China).

Construction of Renal Denervation

Surgical and chemical RDN have been described and applied in our previous study.⁹ Briefly, after the bilateral renal arteries were approached, all visible nerves on the surface of the renal arteries were cut off, and the surrounding renal artery was moistened with a 20% phenol solution for 8–10 min.

HIGHLIGHTS

- Sympathetic activation and gap junction remodeling were found in high-pacing-induced heart failure.
- Renal denervation suppressed sympathetic hyperactivity in high-pacing-induced heart failure.
- Renal denervation alleviates arrhythmia substrate through reduced Cx40 expression and the Cx40/Cx43 ratio in high-pacing-induced heart failure dogs.

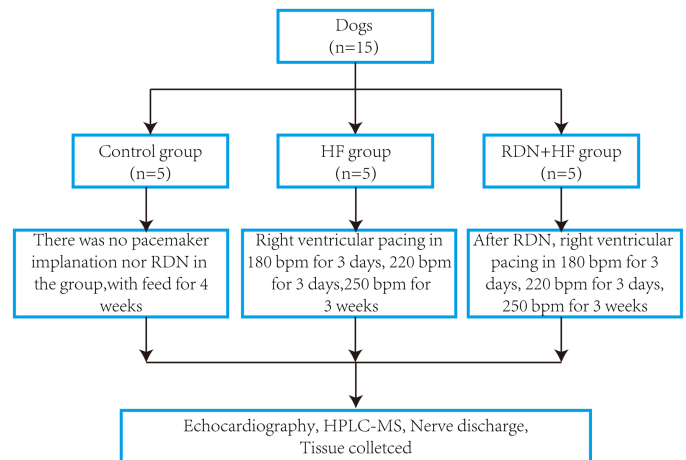


Figure 1. Flowchart of study. Fifteen dogs were randomly divided into control group, heart failure (HF) group, and renal denervation (RDN) + HF group. Right ventricular pacing was used to construct a chronic heart failure model in the HF group. Pacing frequency 180 beats/min for 3 days, pacing frequency 220 beats/min for 3 days, pacing frequency 250 beats/min for 3 weeks. The control group was a sham operation group, no pacemaker implantation, and no RDN surgery was performed. In the RDN+ HF group, after RDN surgery, a pacemaker was implanted to construct heart failure, with a pacing frequency of 180 times/min for 3 days, a pacing frequency of 220 times/min for 3 days, and a pacing frequency of 250 times/min for 3 weeks. Finally, cardiac ultrasound, high-performance liquid chromatography–mass spectrometry were used to detect norepinephrine and epinephrine nerve discharge. Cardiac tissue was collected in the 3 groups for pathological analysis, immunohistochemistry, and Western Blot, and electron microscopy.

Echocardiography

Echocardiography was performed using a phased-array system (Sonos5500, Philips Ultrasound, United States) in the conscious state. The left ventricular EF was recorded after 4-week RVP.

High-Performance Liquid Chromatography–Mass Spectrometry

Our previous study measured norepinephrine (NE) and epinephrine (E) using HP-LC-MS. First, 12.2 mg of E standard (Zhongshan Golden Bridge, China) and 10.0 mg of NE (Zhongshan Golden Bridge, China) were added to 0.1% ascorbic acid solution (1 mg of ascorbic acid was dissolved in 1 mL methanol). The plasma samples (250 µL) were then pretreated with 250 µL of ammonium acetate, 200 µL of methanol, and 200 µL of water, and the sample was dissolved in 200 µL of ammonium acetate and 200 µL of acetonitrile: isopropanol (50 : 50). The samples were blown dry using a nitrogen gun and reconstituted with 50 µL of an acetonitrile: water (85 : 15) solution containing 2% formic acid. Finally, the injection volume was 20 µL for both the sample and the standard. Analysis was performed using ultra-high-performance liquid chromatography (ACQUITY UPLC, Waters) and mass spectrometry (ACQUITY TQD, Waters). Samples were eluted using a gradient program consisting of mobile phase

A, containing 30 mM formic acid in 5 : 95 acetonitrile: MilliQ water, and mobile phase B, containing 30 mM formic acid in 85 : 15 acetonitrile: MilliQ water. The following MS conditions were used: flow rates of cone gas and desolvation gas were 150 and 900 L/h, respectively, with a source temperature of 150°C, desolvation temperature of 550 °C, and Electrospray ionization (ESI⁺).

Nerve Discharge Recording

The left stellate ganglion (LSG) was dissected and the surrounding fat tissue was separated using a glass needle. A pair of silver bipolar microelectronics was inserted into the LSG, and a ground wire was connected to the chest wall to reduce noise. Nerve signals and electrocardiography (ECG) were recorded using the PowerLab data acquisition system in the control and HF group, and all data were analyzed using Lab Chart 8.0/proV7 software (Bio Amp; ADInstruments). The nerve discharge was quantitatively analyzed using signal-to-noise ratios greater than 3:1, as shown in a previous study.¹⁰ The amplitude and frequency of discharge in the 1 minutes were defined as nerve activity.

The ILSG was dissected and the surrounding fat tissue was separated using a glass needle. A pair of silver bipolar microelectronics was inserted into the LSG, and a ground wire was connected to the chest wall to reduce noise. Nerve signals and ECG were recorded using the PowerLab data acquisition system in the control and HF group, and all data were analyzed using Lab Chart 8.0/proV7 software (Bio Amp; ADInstruments). The nerve discharge was quantitatively analyzed using signal-to-noise ratios greater than 3 : 1, as shown in a previous study.¹⁰ The amplitude and frequency of discharge in the 1 minute were defined as nerve activity.

Pathological Analysis

Ventricular tissues were harvested for Masson and Sirius scarlet staining. The area of the interstitial fibers was calculated using image analysis software (ImageJ). The renal arteries were harvested for further hematoxylin staining to observe the renal nerve.

Immunohistochemistry

Paraffin-embedded tissue (renal and myocardial tissues) sections were deparaffinized, baked, dewaxed, and hydrated. The process of immunohistochemical staining was performed as follows: endogenous peroxidase activity was quenched using 3% hydrogen peroxide, samples were subjected to heat-mediated antigen retrieval (citrate buffer, pH 6), and samples were then blocked with goat serum. Primary antibody incubation was performed overnight at 4°C using different dilutions, including tyrosine hydroxylase (TH, 1 : 500, Proteintech, USA), choline acetyltransferase (ChAT, 1 : 300, Bioss, China), connexin (Cx)43 (1 : 500, Abcam, USA), and Cx40 (1 : 200, Abcam, USA) antibodies, and the secondary antibody was incubated for 1 hour at 37°C. The sections were washed 3 times (5 min/wash) after each step. Diaminobenzidine (DAB; ZSGB-BIO, China) was used to stain the sections. Finally, an optical microscope (Leica, Wetzlar, Germany) was used for evaluation. Five fields were selected randomly from each slide for quantitation with Image-J software. The nerve density was calculated as positive nerve

area/total area ×100%. The Cx43, Cx40 expression was calculated as the percentage of Cx43-/Cx40- positive staining area, and Cx43 lateralization was analyzed as in a previous study.¹¹

Western Blot

Western blotting was performed using standard methods, and the ventricles were dissected and subjected to membrane protein extraction. Immunoblot analysis was performed using anti-Cx43 (1 : 1000, Abcam, USA), anti-Cx40 (1 : 1000, Abcam, USA), and GAPDH (1 : 2000, Chemicon, USA). The bands were analyzed by Bio-Image and signal quantitative molecular image chemical DocXRS system analysis (Bio-Rad, Richmond, Calif, USA). As reported previously, band intensities were expressed relative to those of GAPDH.¹¹

Transmission Electron Microscopy

The morphology of the intercalated discs in the ventricle was observed using transmission electron microscopy (TEM, JEM-1220, JEOL Ltd., Tokyo, Japan). Myocardial tissue was fixed with 4% glutaraldehyde for 24 hours, dehydrated with a graded ethanol series, post-fixed with 0.5% osmium tetroxide, contrasted with 2% uranyl acetate and 0.1% tannic acid, and embedded in epoxy resin.¹²

Statistical Analysis

Continuous data are presented as mean ± SD, Kolmogorov–Smirnov tests were performed for checking data normality. Comparisons between 2 groups were carried out using the independent *t* test. Multiple comparisons were evaluated by one-way ANOVA followed by Tukey's Post Hoc multiple comparisons. SPSS 19.0 software (SPSS Inc., Chicago, Ill, USA) was used for data analysis, and statistical significance was defined as *P* < .05.

RESULTS

Renal Denervation Effectively Removed Renal Nerves

As shown in Figure 2A, RDN effectively removed renal nerves. Compared with the control group, the TH-positive area of the renal tissue in the HF group was significantly increased (Figure 2B; Control vs. HF group, *P* = .0052). Compared with the HF group, the TH-positive area of the renal tissue in the RDN+HF group was significantly reduced, indicating that RDN effectively removed renal nerves (Figure 2B; HF vs. RDN+HF group, *P* = .0006).

Successfully Generation of High-Pacing-Induced Heart Failure Model

After 4 weeks of RVP, the HF group had reduced EF (Table 1) (HF group, EF, 40.32 ± 6.09%). Sirius scarlet and Masson staining showed myocardial interstitial fibrosis in the HF group (Figure 3; Sirius scarlet, Control vs. HF group, *P* < .0001; Masson, Control vs. HF group, *P* < .0001). Moreover, plasma BNP was significantly increased in the HF group (Control vs. HF group, 128.6 ± 29.87 vs. 266 ± 48.43, *P* < .0001) (Table 1), indicating that the dog model of HF was successfully established.

Renal Denervation-Alleviated Myocardial Fibrosis

Fibrosis occurred in the ventricles of the HF group according to Sirius scarlet and Masson staining (Figure 3A-B).

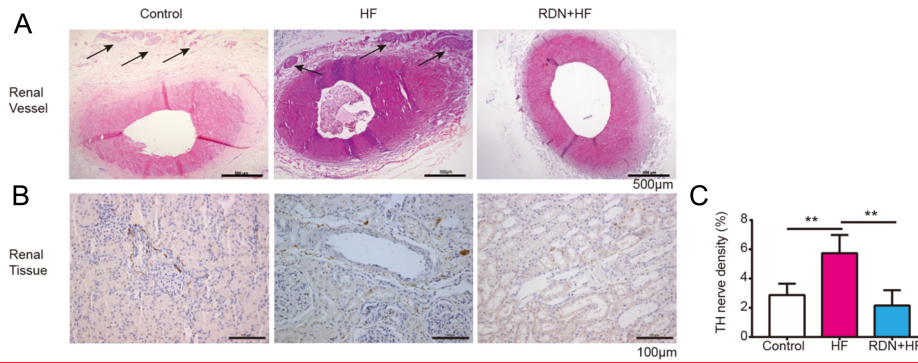


Figure 2. Renal denervation effectively removed renal nerves. (A) Representative images of hematoxylin staining of renal vessels. (B) Representative images of TH staining of renal tissue among 3 groups. (C) Quantitative analysis of TH expression of the renal tissue among 3 groups, *P* < .01. n = 5 for each group.**

Table 1. Echocardiographic Examination and Serum B-type Natriuretic Peptide at 4-Week Rapid Ventricular Pacing

	Control (n=5)	HF (n=5)	RDN+HF (n=5)	<i>P</i>
RV diameter, mm	21.62 ± 1.77	26.4 ± 2.26**	21.84 ± 1.56##	<.05
LVDd, mm	34.77 ± 2.93	41.44 ± 3.50**	38.77 ± 3.47	<.05
LVDs, mm	22.06 ± 2.10	38.25 ± 3.89**	33.02 ± 2.30***	<.01
LVPWd, mm	9.83 ± 0.62	6.46 ± 0.99**	7.86 ± 0.68***	<.01
LVPWs, mm	11.14 ± 0.62	8.61 ± 0.77**	9.10 ± 1.42**	<.01
LVEF, %	66.29 ± 5.74	40.32 ± 6.09**	50.06 ± 2.95***	<.01
BNP, ng/L	128.6 ± 29.87	266 ± 48.43**	174 ± 11.58##	<.01

BNP, B-type Natriuretic Peptide; HF, heart failure; LVDs, left ventricular end systolic diameters; LVDd, left ventricular end diastolic diameter; LVEF, left ventricular ejection fraction; LVPWs, left ventricular posterior wall in systole; LVPWd, left ventricular posterior wall in diastole; RV, right ventricular end-diastolic diameter.

**P* < .05 vs. control.
 ***P* < .01 vs. control.
 #*P* < .05 vs. HF group.
 ##*P* < .01 vs. HF group.

A small amount of fat cell infiltration was observed in the ventricle in the HF group (Figure 3A). Renal denervation-reduced fibrosis of the ventricle (Figure 3A-B; Sirius scarlet, HF vs. RDN+HF group, *P* < .0001; HF vs. RDN+HF group, *P* < .0001).

Renal Denervation-Ameliorated Sympathetic Hyperactivity

Compared to the control group, frequent and amplitude premature ventricular contractions were observed in the HF group, accompanied by an increase in LSG nerve discharges (Figure 4A; frequent, control vs. HF group, *P* < .0001; amplitude, control vs. HF group, *P* < .0001). Epinephrine and NE levels were higher in the HF group than in the control group (Figure 4B; E, control vs. HF, *P* = .0001; NE, control vs. HF, *P* = .0037). Renal denervation suppressed E and NE compared to those in the HF group (Figure 4B; E, HF vs. RDN+HF, *P* = .0001; NE, HF vs. RDN+HF, *P* = .0106). A higher expression of TH-positive nerve densities was observed in the HF group than in the control group (Figure 5A; *P* = .0050), which was reversed by RDN (Figure 5A; *P* = .0070). However, there was no significant difference in ChaT expression in ventricle among the 3 groups (Figure 5B; control vs. HF group, *P* = .4706; control vs. RDN+HF group, *P* = .5191; HF vs. RDN+HF group, *P* = .9959).

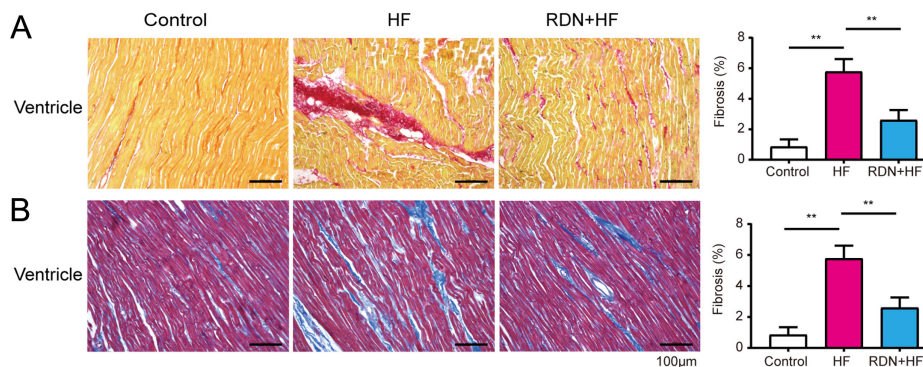


Figure 3. Renal denervation-attenuated ventricular myocardial fibrosis in high-pacing-induced heart failure dogs. (A) Representative Masson staining in ventricle among the 3 groups, and quantitative analysis of the fibrosis in the ventricle. (B) Representative Sirius Scarlet staining ventricle among the groups, Quantitative analysis of fibrosis in the ventricle. **P* < .05, *P* < .01. n = 5 for each group; scale bar, 100 μm.**

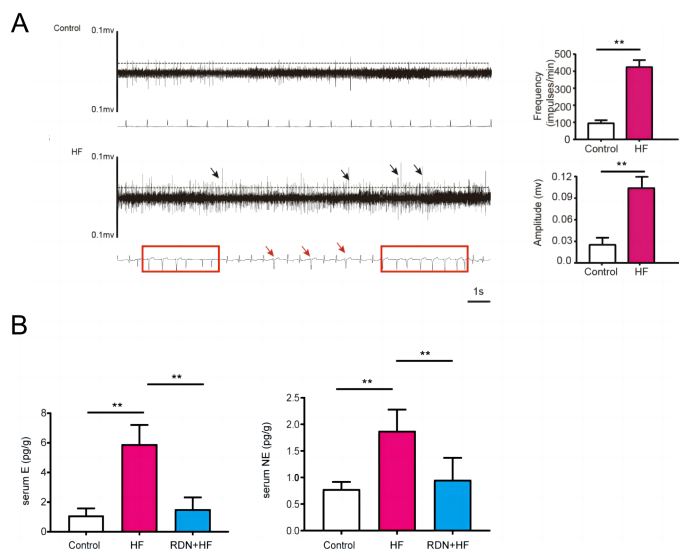


Figure 4. Sympathetic activation in high-pacing-induced heart failure dogs. (A) ECG and LSG nerve discharge. Ventricular extrasystoles are indicated with red arrows, ventricular tachycardia are indicated by red boxes. Black arrows indicate increasing amplitude of sympathetic discharge. ECG, electrocardiography; LSG, left stellate ganglion; scale bar, 1 second. (B) Quantitative analysis of E and NE among 3 groups by HP-LC-MS. E, epinephrine; HP-LC-MS, high-performance liquid chromatography–mass spectrometry; NE, norepinephrine. **P* < .05, *P* < .01. n = 5 for each group.**

Renal Denervation-Alleviated Gap Junction Remodeling in Ventricle

Compared with the control group, the expression of Cx43 in the HF group was significantly reduced (Figure 6A; *P* = .0160); Compared with the HF group, the expression of Cx43 in the RDN+HF group was significantly increased (Figure 6A; *P* = .0013). The lateralization of Cx43 in the HF group was higher than that in the control group (Figure 6A; black arrowheads indicate Cx43 lateralization, *P* < .0001). But, there were no significant differences among the HF and RDN+HF groups for Cx43 lateralization (Figure 6A; black arrowheads indicate Cx43 lateralization, *P* = .0610). Cx40 expression in the HF group was higher than that in

the control group (Figure 6B; *P* = .0010). Cx40 expression in the RDN+HF group was lower than that in the HF group (Figure 6B; *P* = .0488).

Quantitative analysis of the expression of Cx43, Cx40, and Cx40/Cx43 was performed by western blotting (Figure 6C-D). Compared with the control group, Cx43 in the HF group (Figure 6D; *P* = .0004) was significantly reduced, whereas Cx40 expression (Figure 6D; *P* = .0140) and Cx40/Cx43 (Figure 6D; *P* = .0001) ratios were significantly increased. Compared with the HF group, Cx43 in the RDN+HF group increased significantly (Figure 6D; *P* = .0407), and the RDN+HF group showed significantly reduced Cx40 expression (Figure 6D; *P* = .0120) and the ratio of Cx40/Cx43 (Figure 6D; *P* = .0050). In addition, the gap junction and desmosomes connection in the control group were arranged intermittently, but this phenomenon was less frequently seen in the HF group (Figure 6E). Renal denervation seemed to alleviate gap junction remodeling (Figure 6E).

DISCUSSION

Excessive activation of the sympathetic nervous system and changes in gap junction structure play a key role in the development of arrhythmias in HF. Our research uncovered that RDN could potentially improve the arrhythmia-prone environment by mitigating sympathetic overactivation and remodeling of gap junctions in high-pacing-induced HF. The impact of RDN on gap junction remodeling was characterized by a decrease in the levels of Cx40 and the Cx40/Cx43 ratio, alongside an increase in Cx43 expression.

Sympathetic Activation in High-Pacing-Induced Heart Failure

The significant role of the sympathetic nervous system in the development and persistence of arrhythmia has been well established. Studies have demonstrated that heightened sympathetic activity extends repolarization duration, enhances repolarization variability, and elevates the rate of arrhythmia.¹⁰ In cases of HF, there is an initial rise in cardiac sympathetic nerve activity, precipitating ventricular arrhythmias.^{13,14} Our research similarly indicated that ventricular contractions associated with sympathetic overactivation were observed in high-pacing-induced HF dogs.

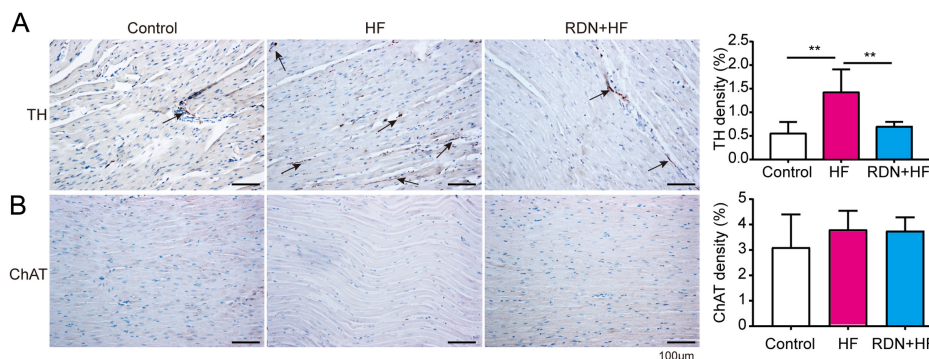


Figure 5. Effects of renal denervation on autonomic neural remodeling. (A) Representative images and quantitative analysis of TH staining. (B) Representative images and quantitative analysis of ChAT staining. **P* < .05, *P* < .01. n = 5 for each group; scale bar, 100 μm.**

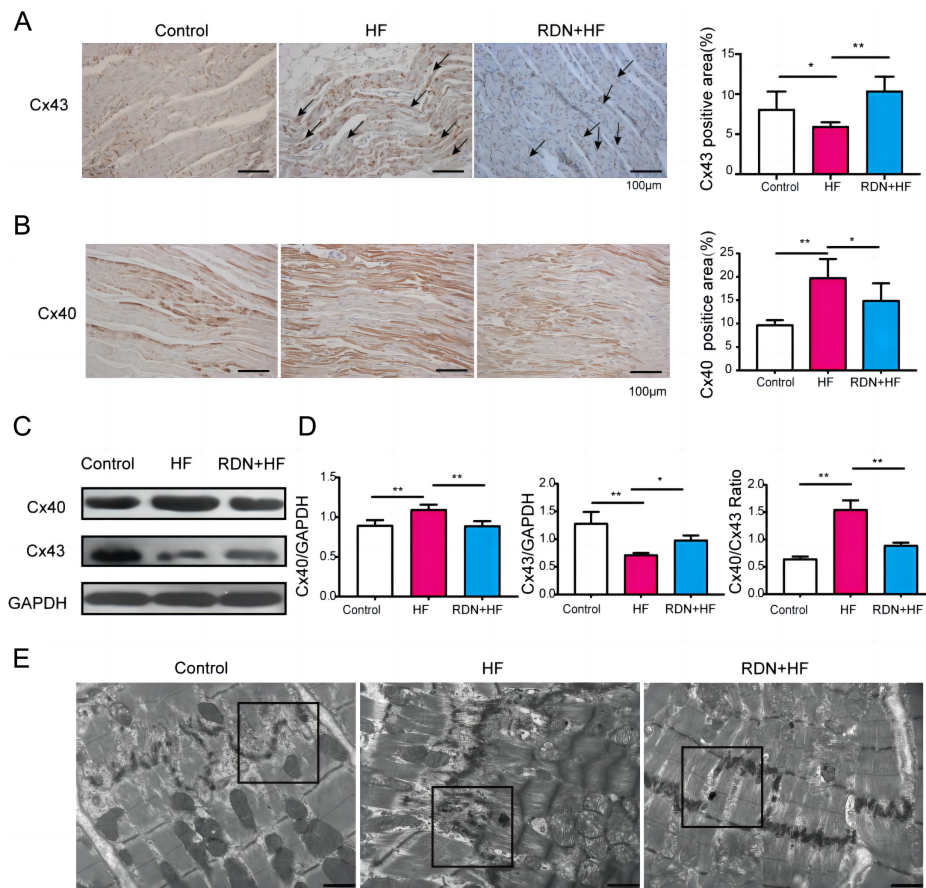


Figure 6. Effects of renal denervation on gap junction remodeling. (A) Immunohistochemical staining of Cx43 on the ventricle. A black row indicates the Cx43 lateralization. (B) Immunohistochemical staining of Cx40 on the ventricle. (C) Expression of Cx40 and Cx43 was detected by western blotting. (D) Quantitative analysis of the expression levels of Cx43, Cx40, and Cx40/Cx43 ratio. * $P < .05$, ** $P < .01$; $n = 5$ for each group. Cx43, connexin 43; Cx40, connexin 40. (E) Ultrastructural images of gap junction in the ventricular myocardium conducted by transmission electron microscopy; The region of the gap junction is indicated by the black box; scale bar, 1 μm.

Renal Denervation-Suppressed Sympathetic Hyperactivity in High-Pacing-Induced Heart Failure

Renal denervation is a novel intervention strategy for autonomic nerve regulation. It not only suppresses the activity of sympathetic nerves but also reduces the activity of the RASS system.¹⁵ Renal denervation shows promise for patients with atrial fibrillation (AF) stemming from both pulmonary vein and extrapulmonary vein triggers.¹⁶ The ERADICATE-AF study demonstrated a notable decrease in the recurrence rate of AF and atrial tachyarrhythmias in patients who underwent RDN alongside circumflex pulmonary vein isolation.¹⁷ Nevertheless, further validation through extensive long-term trials is necessary to confirm these findings. In 2018, our team found that RDN reduces ventricular arrhythmia after myocardial infarction by reducing the sympathetic activity.⁹ Yamada et al¹⁴ also suggested that RDN reduced the risk of ventricular arrhythmia (manifested in the shortening of ERP and reduction of APD₉₀) in a rabbit model of HF by inhibiting sympathetic activity.^{14,18} On the other hand, a study conducted by Evranos et al¹⁹ has demonstrated that RDN is a secure and efficient method for decreasing the arrhythmia load in individuals with stubborn ventricular arrhythmias.

Additionally, it has the potential to serve as a treatment option for polymorphic ventricular tachycardia that triggers electrical storms.^{19,20} In our study, RDN reduced the sympathetic activity and NE/E. Further, the changes of vagus nerves in the ventricles were not significant in this study. This finding suggests that RDN reduces the risk of ventricular arrhythmia in HF possibly mainly by suppressing sympathetic activity. This further demonstrated that arrhythmia connected with the activation of sympathetic.

Renal Denervation-Regulated Cardiac Fibrosis

Numerous research studies have indicated that there is obvious atrial and ventricular fibrosis in HF. Myocardial fibrosis results in slow conduction and increased heterogeneity.^{21,22} Li et al²³ found that RDN reduced atrial and ventricular fibrosis in HF after myocardial infarction. Consistent with prior studies,²⁴ our study demonstrated that RDN inhibited myocardial fibrosis and improved cardiac function in high-pacing-induced HF dogs.

Renal Denervation-Regulated Gap Junction Remodeling

Gap junction mediates intercellular electrical coupling in cardiomyocytes. The gap junction proteins found in the heart,

Cx40 and Cx43, have been strongly linked to arrhythmias. Studies have found that a decrease in Cx43 expression leads to uncoupling of the gap junction, ultimately increasing the risk of ventricular arrhythmias. Additionally, the presence of Cx40 in myocardial tissue is inversely related to gap junction conduction velocity. Our research demonstrated that RDN resulted in an increase in Cx43 expression and a decrease in Cx40 expression. Previous literature has indicated that activation of sympathetic nerves or the RAAS can lead to downregulation of Cx43 and upregulation of Cx40 in the heart. Our findings further support the association between sympathetic nerve activity and the expression levels of Cx43 and Cx40. Therefore, it is plausible to suggest that RDN may impact arrhythmia susceptibility by modulating the expression of Cx40 and Cx43.

The ratio of Cx40 to Cx43 is correlated with the development of arrhythmia. When increasing Cx40/Cx43 ratio results in decreased coupling, consequently reducing conduction speed between cardiomyocytes and elevating the risk of reentrant arrhythmia.^{25,26} The alteration in the Cx40/Cx43 ratio is partially initiated by the signaling cascade in the extracellular matrix (involving cAMP, angiotensin II, and growth factors).²⁷ Our research demonstrated that RDN led to decreased levels of the Cx40/Cx43 ratio. We believe that this effect may stem from RDN's influence on the RAAS or sympathetic nervous system activity.

Lateralized Cx43 was located on both sides of the cell boundary. Connexin 43 lateralization in HF has been shown in this study. Connexin 43 lateralization leads to increased propensity for arrhythmogenesis. The possible reasons for this might include the following 3 reasons: i) Lateralized Cx43 may lose its original function and lack mechanical stability.^{28,29} ii) Cx43 lateralization has been associated with decreased longitudinal conduction velocity (a potential proarrhythmic change).³⁰⁻³² 3. Zigzag conduction is caused by the lateralization of Cx43.^{5,33} Previous studies have shown that Cx43 lateralization is directly attributed to sympathetic overactivation via adrenergic receptor agonists.³⁴ Yet this study did not show RDN-reduced Cx43 lateralization. This result could be attributed to multiple possible reasons: first, a relatively short follow-up period. Second, Cx43 lateralization may be regulated by multiple system control mechanisms, such as autophagy, mechanical overload. Given that Cx43 lateralization can also be arrhythmogenic, how to reduce the lateralization of Cx43 needs to be further studied.

Study Limitations

This study has some limitations. First, the exact mechanism of RDN altering gap junction remodeling is not clear. Second, the ways of reducing lateralization of Cx43 were unclear.

CONCLUSION

Sympathetic hyperactivity and gap junction remodeling have been observed in high-pacing-induced HF dogs. Renal denervation-reduced sympathetic activity, Cx40 expression, and the Cx40/Cx43 ratio in high-pacing-induced HF dogs.

Data Availability: The datasets generated or analyzed during this study are available from the corresponding author on reasonable request.

Ethics Committee Approval: The study was approved by the Ethics Committee of the First Affiliated Hospital of Xinjiang Medical University (IACUC-201902-K03) on February 14, 2019.

Informed Consent: Not applicable.

Peer-review: Externally peer-reviewed.

Author Contributions: Concept – Y.L., B.T.; Design – X.L., B.T.; Supervision – Z.B., Y.L.; Resources – Z.B., Y.L.; Materials – Q.W., X.Z.; Data Collection and/or Processing – X.L., S.S.; Analysis and/or Interpretation – X.L., J.X.; Literature Search – X.L., H.L.; Writing – X.L., S.S.; Critical Review – Z.B., Y.F., X.Z.

Declaration of Interests: The authors declare that the research was conducted in the absence of any commercial or financial relationships that could be construed as potential conflicts of interest.

Funding: This study was supported by the top young scientific and technological talents of Tianshan Talent Cultivation Program in (project number: 2022TSYCCX0101), Basic scientific research business funds for colleges and universities (project number: XJEDU2023P066). Sponsored by Natural Science Foundation of Xinjiang Uygur Autonomous Region (2023D01C44).

REFERENCES

- Ren L, Wu C, Yang K, et al. A disintegrin and Metalloprotease-22 attenuates hypertrophic remodeling in mice through inhibition of the protein kinase B signaling pathway. *J Am Heart Assoc.* 2018;7(2). [CrossRef]
- Lou Q, Janks DL, Holzem KM, et al. Right ventricular arrhythmogenesis in failing human heart: the role of conduction and repolarization remodeling. *Am J Physiol Heart Circ Physiol.* 2012;303(12):H1426-H1434. [CrossRef]
- Wang Y, Hill JA. Electrophysiological remodeling in heart failure. *J Mol Cell Cardiol.* 2010;48(4):619-632. [CrossRef]
- Akar FG, Nass RD, Hahn S, et al. Dynamic changes in conduction velocity and gap junction properties during development of pacing-induced heart failure. *Am J Physiol Heart Circ Physiol.* 2007;293(2):H1223-H1230. [CrossRef]
- Imanaga I. Pathological remodeling of cardiac gap junction connexin 43-With special reference to arrhythmogenesis. *Pathophysiology.* 2010;17(2):73-81. [CrossRef]
- Beauchamp P, Yamada KA, Baertschi AJ, et al. Relative contributions of connexins 40 and 43 to atrial impulse propagation in synthetic strands of neonatal and fetal murine cardiomyocytes. *Circ Res.* 2006;99(11):1216-1224. [CrossRef]
- Salameh A, Krautblatter S, Karl S, et al. The signal transduction cascade regulating the expression of the Gap junction protein connexin43 by beta-adrenoceptors. *Br J Pharmacol.* 2009;158(1):198-208. [CrossRef]
- Powers JC, Recchia F. Canine model of pacing-induced heart failure. *Methods Mol Biol.* 2018;1816:309-325. [CrossRef]
- Zhang WH, Zhou QN, Lu YM, et al. Renal denervation reduced ventricular arrhythmia after myocardial infarction by inhibiting sympathetic activity and remodeling. *J Am Heart Assoc.* 2018;7(20):e009938. [CrossRef]
- Wang J, Dai M, Cao Q, et al. Carotid baroreceptor stimulation suppresses ventricular fibrillation in canines with chronic heart failure. *Basic Res Cardiol.* 2019;114(6):41. [CrossRef]

11. Burstein B, Comtois P, Michael G, et al. Changes in connexin expression and the atrial fibrillation substrate in congestive heart failure. *Circ Res*. 2009;105(12):1213-1222. [\[CrossRef\]](#)
12. González E, Rother M, Kerr MC, et al. Chlamydia infection depends on a functional MDM2-p53 axis. *Nat Commun*. 2014;5:5201. [\[CrossRef\]](#)
13. Yamada S, Fong MC, Hsiao YW, et al. Impact of renal denervation on atrial arrhythmogenic substrate in ischemic model of heart failure. *J Am Heart Assoc*. 2018;7(2). [\[CrossRef\]](#)
14. Yamada S, Lo LW, Chou YH, et al. Renal denervation ameliorates the risk of ventricular fibrillation in overweight and heart failure. *Europace*. 2020;22(4):657-666. [\[CrossRef\]](#)
15. Hoogerwaard AF, Elvan A. Is renal denervation still a treatment option in cardiovascular disease? *Trends Cardiovasc Med*. 2020;30(4):189-195. [\[CrossRef\]](#)
16. Şaylık F, Çınar T, Akbulut T, Hayıroğlu Mİ. Comparison of catheter ablation and medical therapy for atrial fibrillation in heart failure patients: a meta-analysis of randomized controlled trials. *Heart Lung*. 2023;57:69-74. [\[CrossRef\]](#)
17. Nesapiragasan V, Hayıroğlu Mİ, Sciacca V, Sommer P, Sohns C, Fink T. Catheter ablation approaches for the treatment of arrhythmia recurrence in patients with a durable pulmonary vein isolation. *Balk Med J*. 2023;40(6):386-394. [\[CrossRef\]](#)
18. Zandstra TE, Notenboom RGE, Wink J, et al. Asymmetry and heterogeneity: part and parcel in cardiac autonomic innervation and function. *Front Physiol*. 2021;12:665298. [\[CrossRef\]](#)
19. Evranos B, Canpolat U, Kocyigit D, Coteli C, Yorgun H, Aytemir K. Role of adjuvant renal sympathetic denervation in the treatment of ventricular arrhythmias. *Am J Cardiol*. 2016;118(8):1207-1210. [\[CrossRef\]](#)
20. Prado GM, Mahfoud F, Lopes RD, et al. Renal denervation for the treatment of ventricular arrhythmias: a systematic review and meta-analysis. *J Cardiovasc Electrophysiol*. 2021;32(5):1430-1439. [\[CrossRef\]](#)
21. Chen WJ, Liu H, Wang ZH, et al. The impact of renal denervation on the progression of heart failure in a canine model induced by right ventricular rapid pacing. *Front Physiol*. 2019;10:1625. [\[CrossRef\]](#)
22. Tham YK, Bernardo BC, Ooi JYY, Weeks KL, McMullen JR. Pathophysiology of cardiac hypertrophy and heart failure: signaling pathways and novel therapeutic targets. *Arch Toxicol*. 2015;89(9):1401-1438. [\[CrossRef\]](#)
23. Li HG, Jones DL, Yee R, Klein GJ. Electrophysiologic substrate associated with pacing-induced heart failure in dogs: potential value of programmed stimulation in predicting sudden death. *J Am Coll Cardiol*. 1992;19(2):444-449. [\[CrossRef\]](#)
24. Lu Y, Sun J, Zhou X, Zhang L, Ma M, Tang B. Effect of low-level vagus nerve stimulation on cardiac remodeling in a rapid atrial pacing-induced canine model of atrial fibrillation. *J Cardiovasc Pharmacol*. 2016;67(3):218-224. [\[CrossRef\]](#)
25. Kanagaratnam P, Rothery S, Patel P, Severs NJ, Peters NS. Relative expression of immunolocalized connexins 40 and 43 correlates with human atrial conduction properties. *J Am Coll Cardiol*. 2002;39(1):116-123. [\[CrossRef\]](#)
26. Wang X, Zhao Q, Huang H, et al. Effect of renal sympathetic denervation on atrial substrate remodeling in ambulatory canines with prolonged atrial pacing. *PLoS One*. 2013;8(5):e64611. [\[CrossRef\]](#)
27. Yamada K, Green KG, Samarel AM, Saffitz JE. Distinct pathways regulate expression of cardiac electrical and mechanical junction proteins in response to stretch. *Circ Res*. 2005;97(4):346-353. [\[CrossRef\]](#)
28. Solan JL, Lampe PD. Spatio-temporal regulation of connexin43 phosphorylation and gap junction dynamics. *Biochim Biophys Acta Biomembr*. 2018;1860(1):83-90. [\[CrossRef\]](#)
29. Fontes MSC, van Veen TAB, de Bakker JMT, van Rijen HVM. Functional consequences of abnormal Cx43 expression in the heart. *Biochim Biophys Acta*. 2012;1818(8):2020-2029. [\[CrossRef\]](#)
30. Akar FG, Spragg DD, Tunin RS, Kass DA, Tomaselli GF. Mechanisms underlying conduction slowing and arrhythmogenesis in nonischemic dilated cardiomyopathy. *Circ Res*. 2004;95(7):717-725. [\[CrossRef\]](#)
31. Poelzing S, Rosenbaum DS. Altered connexin43 expression produces arrhythmia substrate in heart failure. *Am J Physiol Heart Circ Physiol*. 2004;287(4):H1762-H1770. [\[CrossRef\]](#)
32. Uzzaman M, Honjo H, Takagishi Y, et al. Remodeling of gap junctional coupling in hypertrophied right ventricles of rats with monocrotaline-induced pulmonary hypertension. *Circ Res*. 2000;86(8):871-878. [\[CrossRef\]](#)
33. Severs NJ, Bruce AF, Dupont E, Rothery S. Remodelling of gap junctions and connexin expression in diseased myocardium. *Cardiovasc Res*. 2008;80(1):9-19. [\[CrossRef\]](#)
34. Xia Y, Gong KZ, Xu M, et al. Regulation of gap-junction protein connexin 43 by beta-adrenergic receptor stimulation in rat cardiomyocytes. *Acta Pharmacol Sin*. 2009;30(7):928-934. [\[CrossRef\]](#)